JGR Biogeosciences

RESEARCH ARTICLE
10.1029/2018JG004804

Plant Feedback Aggravates Soil Organic Carbon Loss Associated With Wind Erosion in Northwest China

Lingjie Lei[1], Kesheng Zhang[1], Xuanze Zhang[2,3], Ying-Ping Wang[4,5], Jianyang Xia[2,3], Shilong Piao[6,7,8], Dafeng Hui[9], Mingxing Zhong[1], Jingyi Ru[1], Zhenxing Zhou[1], Hongquan Song[1], Zhongling Yang[1], Dong Wang[1], Yuan Miao[1], Fan Yang[1], Bin Liu[1], Ang Zhang[1], Mengyang Yu[1], Xianghui Liu[1], Yongheng Song[1], Lili Zhu[1], and Shiqiang Wan[1,10]

[1]International Joint Research Laboratory for Global Change Ecology, College of Life Sciences, Henan University, Kaifeng, Henan, China, [2]Research Center for Global Change and Ecological Forecasting, School of Ecological and Environmental Science, East China Normal University, Shanghai, China, [3]Institude of Eco-Chongming (IEC), Shanghai, China, [4]CSIRO Oceans and Atmosphere, Aspendale, Victoria, Australia, [5]South China Botanical Garden, Chinese Academy of Sciences, Guangzhou, China, [6]Sino-French Institute for Earth System Science, College of Urban and Environmental Sciences, Peking University, Beijing, China, [7]Key Laboratory of Alpine Ecology and Biodiversity, Institute of Tibetan Plateau Research, Chinese Academy of Sciences, Beijing, China, [8]Center for Excellence in Tibetan Earth Science, Chinese Academy of Sciences, Beijing, China, [9]Department of Biological Sciences, Tennessee State University, Nashville, TN, USA, [10]College of Life Science, Hebei University, Baoding, Hebei, China

Key Points:
- Wind erosion affects soil organic carbon storage through physical process and plant feedback
- Reductions of carbon input from plant biomass to soil due to soil nitrogen loss aggravate soil organic carbon loss
- Plant feedback associated with wind erosion should be considered in assessing soil organic carbon storage

Supporting Information:
- Supporting Information S1

Correspondence to:
S. Wan,
swan@ibcas.ac.cn

Citation:
Lei, L., Zhang, K., Zhang, X., Wang, Y.-P., Xia, J., Piao, S., et al. (2019). Plant feedback aggravates soil organic carbon loss associated with wind erosion in northwest China. *Journal of Geophysical Research: Biogeosciences*, *124*, 825–839. https://doi.org/10.1029/2018JG004804

Received 14 SEP 2018
Accepted 7 MAR 2019
Accepted article online 18 MAR 2019
Published online 6 APR 2019

Abstract Soil organic carbon (SOC) loss caused by wind erosion can profoundly impact carbon (C) balance in arid and semiarid regions. Nevertheless, previous researches mainly focused on the direct effect of wind erosion through removing surface soil only but ignored its indirect effects associated with soil nitrogen (N) loss and subsequent reductions of plant productivity. To better understand the wind erosion effect on SOC storage, we conducted a large-scale field experiment by manipulating wind erosion at 371 sites in arid and semiarid regions of northwest China from 2014 to 2016. We further integrated an observation-based empirical equation of wind erosion process into a terrestrial biogeochemical model to evaluate the direct and indirect effects of wind erosion on SOC storage in northwest China. The observed results showed that direct SOC losses increased linearly with the square of wind speed but decreased nonlinearly with soil water content. Over the 34 years (1980–2013), simulated cumulative SOC losses associated with wind erosion in northwest China were 27.47 Tg C, among which the indirect effects contributed to 2.68 Tg C (9.76%). The indirect effect of wind erosion initially enhanced SOC storage by decreasing heterotrophic respiration from 1984 to 1988 but decreased SOC pool by reducing net primary productivity due to soil N loss under the long-term wind erosion scenario. This work, for the first time, quantified the indirect impact of wind erosion on SOC storage via feedback of suppressed plant productivity, which is crucial for the convincing assessment on SOC storage in arid and semiarid regions.

Plain Language Summary Understanding the magnitude of soil organic carbon (SOC) loss caused by wind erosion is beneficial to assess SOC storage in arid and semiarid regions. Through integrating an empirical relationship of direct SOC loss with environmental factors from a large-scale field experiment by manipulating wind erosion into a terrestrial biogeochemical model, we simulated wind erosion effect on SOC storage in northwest China from 1980 to 2013. Results showed that wind erosion not only directly removed SOC but also decreased soil nitrogen content, leading to a reduction of plant productivity, and thus indirectly decreased SOC storage. This study reveals that omitting plant feedback due to soil nitrogen loss could underestimate wind erosion effect on SOC storage.

1. Introduction

Soil is the largest carbon (C) pool (~2,300 Pg C) in global terrestrial biosphere (Batjes, 1996; Lal, 2003). A small change in soil organic C (SOC) storage may lead to a large variation of ecosystem C exchange between the terrestrial biosphere and the atmosphere (Chappell et al., 2016). Wind erosion is one of the natural processes influencing ecosystems, especially in arid and semiarid regions (Shao et al., 2011). For example, wind erosion can both directly and indirectly affect SOC storage (Yan et al., 2005). SOC can be directly removed by wind erosion through displacing soil organic matter from land surface to the atmosphere (e.g., dust

emission), and this physical process-induced SOC loss has been demonstrated by many previous studies (Borrelli et al., 2017; Hagen, 2002; Lal, 2003; Webb et al., 2012). An estimated 2,000-Mt dust is emitted globally by wind erosion (Shao et al., 2011), and thus, omitting SOC losses associated with wind erosion would lead to an overestimation of potential C sink (Chappell et al., 2016). Given the reduction of substrate, heterotrophic respiration (R_h) is indirectly decreased by the direct SOC loss (Bremer & Kuikman, 1994). In addition, wind erosion can indirectly influence SOC storage via plant feedbacks to soil (Gregorich et al., 1998). However, the magnitude of this indirect effect is rarely quantified, posing challenges for the convincing assessment on ecosystem C sequestration in arid and semiarid regions.

Wind erosion leads to losses of not only SOC but also soil nitrogen (N; Li et al., 2004). Given the well-documented limitations of soil N on plant productivity (Lu et al., 2011; Xia & Wan, 2008), soil N loss reduces plant photosynthesis rate (Luo et al., 2004), net primary productivity (NPP; LeBauer & Treseder, 2008; Lu et al., 2011), and subsequently SOC accumulation (Fontaine et al., 2007; Leff et al., 2012; Liu et al., 2009). However, no evidence on how and to what extent the feedback of decreased plant productivity affects SOC storage associated with wind erosion has been reported.

The water-limited ecosystems in northwest China have been well known to suffer from wind erosion (Lal, 2003; Shao et al., 2011; Song et al., 2016). In order to comprehensively evaluate the impacts of wind erosion on soil C storage in this region, we assessed both direct and indirect effects of wind erosion. We first carried out large-scale field experiments at 371 sites in arid and semiarid regions of northwest China during 2014–2016 (Figure 1) and then developed a relationship of direct SOC loss caused by wind erosion with environmental factors. The Community Atmosphere Biosphere Land Exchange (CABLE) model (Wang et al., 2010; Zhang et al., 2013, 2011) was further improved to simulate the feedback of wind erosion-included N-limitation on C storage. The objectives of this study were to (1) estimate the 34-year (1980–2013) direct effect of wind erosion on SOC storage and (2) explore the mechanism and magnitude of indirect effect of wind erosion on SOC storage in northwest China.

2. Materials and Methods

2.1. Sampling Sites and Experimental Design

The arid and semiarid regions in northwest China encompass territories of eight different provinces in China with a total area of 4.64×10^6 km^2 (Figure 1). The mean annual precipitation is below 400 mm in most of the region that is dominated by grassland and desert ecosystems (Song et al., 2016). From 2014 to 2016, extensive field experiments were conducted in northwest China, covering a longitude from 76.3 to 117.5°E and a latitude from 36.1 to 48.2°N. The ecosystem types consist of grasslands, croplands, shrublands, and deserts (Figure 1).

Over the experimental period, 371 sites were selected for studying the effects of wind erosion on SOC storage. Disturbance of wind erosion on soil surface was manipulated by a wind fire extinguisher (Figure S1 in the supporting information). Wind speed was varied by changing the accelerator magnitude of the wind fire extinguisher. The quadrat (1×1 m^2) was surrounded by plastic plate to prevent soil blown out of the quadrat. The $1 \times 1 \times 1$-m^3 wind-proof collection bag was used to collect the soil blown by the wind fire extinguisher. To ensure the uniformity of the wind disturbance, we randomly inserted five rulers into the soil to record the thickness of the soil that was removed by wind. The wind direction was regulated by the angle between the plastic plate on the wind fire extinguisher and the soil surface. In the spring (April and May) of 2014, we controlled the wind speeds at 12, 16, 21, or 25 m/s to disturb the land surface for 30 s at 49 sites in Inner Mongolia. The wind speed and duration were measured using anemograph and chronograph, respectively. To explore the temporal difference of wind erosion effect, we selected 64 sites in Inner Mongolia with the disturbance of 25-m/s wind speed in the autumn (September and October) of 2014. The wind speed was set at 25 m/s to assess the spatial difference of wind erosion effect in five provinces of northwest China in spring of 2015 (84 sites) and 2016 (174 sites). The wind erosion treatment was replicated three times at each site within an adjacent range (10 m).

The soil samples were transferred to the lab to measure SOC content and soil water content (SWC). The SOC content was analyzed by an element analyzer (Vario MACRO cube, Elementar INC., Germany). The SOC content of the soil samples represented the observed SOC loss under the wind erosion treatment. The

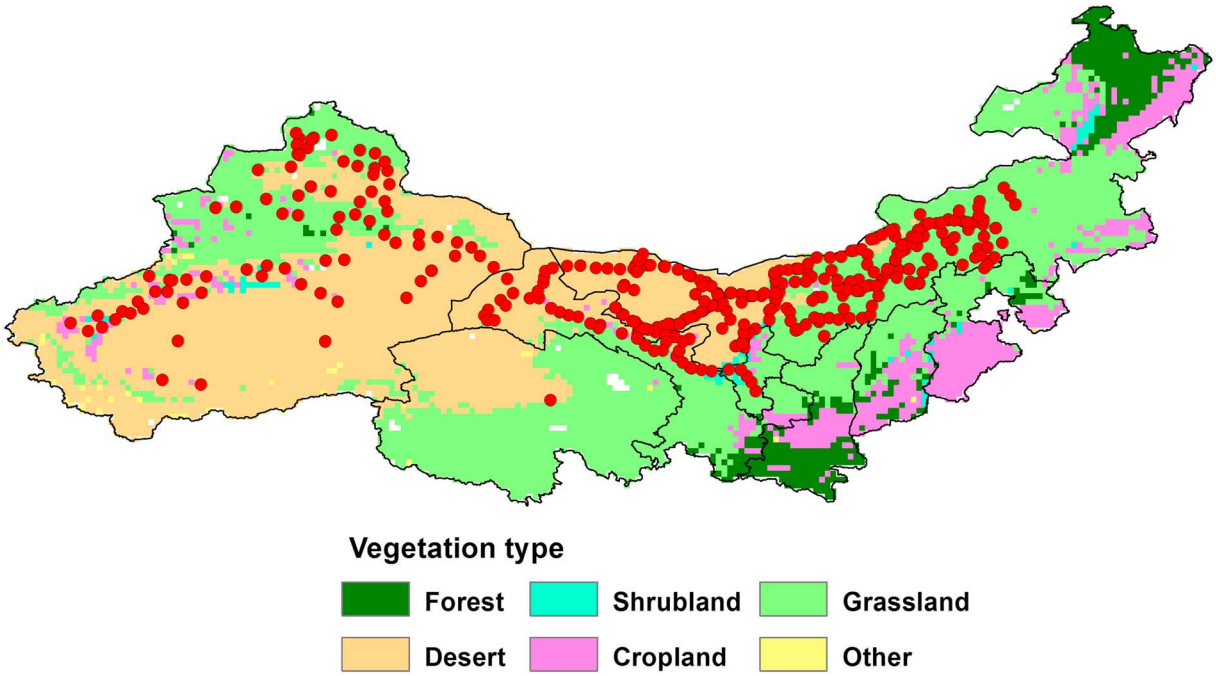

Figure 1. Study area and field sampling sites. Vegetation type is provided by the MODIS product from https://lpdaac.usgs.gov/get_data.

SWC was measured using the gravimetric method. The soil bulk density of soil surface (0–10 cm) was determined at each site. The volumetric water content ($V/V\%$) used in this study was calculated by weight water content and soil bulk density.

2.2. Model Description

The CABLE model is a C-N coupled global land surface model, which has been used to simulate terrestrial biophysical and biogeochemical processes (Wang et al., 2010, 2011). It includes five submodels: canopy radiation, canopy micrometeorology, surface flux, soil and snow, and biogeochemical cycles. The CABLE model simulates both C and N cycles, including effects of N limitation on NPP (C input to soil) and soil microbial respiration (C loss from soil), therefore dynamics of SOC.

The CABLE model has been evaluated by experimental observations (De Kauwe et al., 2017; Zaehle et al., 2014), eddy flux measurements (Best et al., 2015), and satellite data sets (Piao et al., 2015) in many model-data comparison studies. These studies have indicated that the performance of CABLE model is generally consistent with other terrestrial ecosystem models.

2.3. Incorporating Wind Erosion Process Into the CABLE Model

For this study, we simulated the direct effect of wind erosion on SOC storage as the SOC loss (C_{loss}) in each SOC pool (C_{pool}). The arid and semiarid regions in northwest China are important dust sources on the land surface. The dust rose from northwest China mainly influences eastern China, Korea, Japan, and even the Pacific Ocean (Shao et al., 2011; Uno et al., 2009). Previous studies have demonstrated that silt- and clay-size particles (<20 μm) can be always removed by wind erosion (Chen & Fryrear, 2002; Kok, 2011; Li et al., 2004; Webb et al., 2012). Thus, we assumed that the silt and clay (<20 μm) associated soil C and N removed by wind erosion would be deposited outside the model domain, and the sand (>20 μm) associated soil C and N would not be lost by wind erosion and remain in the same grid cell. The C_{pool} under the wind erosion scenario in CABLE model was calculated as

$$C_{pool} = C_{pool} \times sand_c\% + \max\left(0, C_{pool} \times (silt_c\% + clay_c\%) - C_{loss}\right) \quad (1)$$

where $sand_c\%$, $silt_c\%$, and $clay_c\%$ were contributions of organic C in sand, silt, and clay in soil surface to total SOC, respectively. Li et al. (2018) has indicated that contribution of organic C in fine fraction (<20 μm) to total SOC was 54.03%, and thus, $silt_c\%$ plus $clay_c\%$ was 54.03% and $sand_c\%$ was 45.97% in this study.

Direct soil organic N loss (N_{loss}) and soil mineral N loss (Nm_{loss}) by wind erosion were calculated by

$$N_{loss} = C_{loss} \times R_{N/C} \quad (2)$$

$$Nm_{loss} = N_{loss} \times R_{Nm/N} \quad (3)$$

$R_{N/C}$ was defined as the ratio of N and C in soil pool in the CABLE model. $R_{Nm/N}$ was 0.00007 and represented the ratio of soil mineral N and soil organic N, which was observed in a long-term experiment in grassland (Lei et al., 2018; Niu et al., 2011). Thus, the soil organic N pool (N_{pool}) and soil mineral N pool (Nm_{pool}) under wind erosion scenario were expressed as

$$N_{pool} = N_{pool} \times sand_n\% + \max\left(0, N_{pool} \times (silt_n\% + clay_n\%) - N_{loss}\right) \quad (4)$$

$$Nm_{pool} = Nm_{pool} \times sand_n\% + \max\left(0, Nm_{pool} \times (silt_n\% + clay_n\%) - Nm_{loss}\right) \quad (5)$$

where $sand_n\%$, $silt_n\%$, and $clay_n\%$ were the contributions of N in sand, silt, and clay in soil surface to total soil N, respectively. $silt_n\%$ plus $clay_n\%$ was 58.41%, and $sand_n\%$ was 41.59% (Li et al., 2018). Given the N but not phosphorus (P) limitation on plant growth in the study region (Niu et al., 2010; Xia et al., 2009), P loss associated with wind erosion was not considered in this study. Soil C and N losses caused by wind erosion occurred when wind speed was greater than zero. C_{loss}, N_{loss}, and Nm_{loss} would be zero when all slit and clay in soil were removed entirely.

The indirect effect of wind erosion on SOC storage was calculated by the response of plant productivity to N loss under wind erosion scenario. In CABLE model, NPP was calculated as

$$NPP = GPP(L, v_{cmax}, j_{max}) - \sum_i R_{mi}(N_i) - R_g(N/P) \quad (6)$$

where L was the canopy leaf area index, v_{cmax} and j_{max} were the maximum carboxylation rate and maximum rate of potential electron transport of the leaves at the canopy top, respectively, both were dependent on leaf N (g N/m^2) based on the relationship developed by Kattge et al. (2009) for different plant functional types (Wang et al., 2012). R_{mi} and R_g were the maintenance respiration of plant tissue (i = leaf, wood, or root) and growth respiration rate, respectively. R_{mi} was a function of tissue N amount (Zhang et al., 2013). R_g varied with leaf tissue N and P ratio (g N/g P; Zhang et al., 2013). The N concentration in plant tissues (leaf, wood, or root) depended on plant N uptake and the allocation of N uptake among different tissues (Wang et al., 2010). Plant N uptake depended on the demand that was calculated as a function of allocated NPP and optimal tissue $R_{N/C}$ and supply (e.g., available soil mineral N). When supply was lower than demand, plant N uptake was reduced, and leaf tissue $R_{N/C}$ was lowered, so did v_{cmax} and j_{max} thereby NPP. R_h in the CABLE model was the CO_2 release of the decomposition of litter C and SOC (Wang et al., 2011). Net ecosystem productivity represented the difference between NPP and R_h. The C flux from the atmosphere to ecosystem was defined as a positive value and that from ecosystem to the atmosphere was defined as a negative value.

Litter decomposition rate depended on litter quality (lignin:N ratio) and was reduced when litter decomposition was N-limited (Wang et al., 2007). Litter C dynamic (Ld) was calculated as

$$Ld = \tau_{plant} \times C_{plant} - X_{litter} \times \tau_{litter} \times C_{litter} \quad (7)$$

$$X_{litter} = \min\left(1.0, \frac{\tau_{soil} \times C_{soil}}{\tau_{litter} \times C_{litter}} \times \frac{\alpha_{soil}}{0.6\alpha_{soil} - \alpha_{litter}}\right) \quad (8)$$

where τ_{plant}, τ_{litter}, and τ_{soil} were the rate constants for the plant, litter, and soil C pools, respectively. C_{plant}, C_{litter}, and C_{soil} were the size of plant, litter, and soil C pools, respectively. The reduction factor of litter C decomposition (X_{litter}) was limited by the ratio of N and C of soil organic matter (α_{soil}) and plant litter (α_{litter}). Therefore, the decrease of soil N pool by wind erosion limited plant productivity, leading to the reduction of C input from litter to soil and thus indirectly influenced SOC storage in the CABLE model.

2.4. Model Inputs and Simulations

CABLE was driven by the external forcing variables including air temperature, precipitation, downward shortwave radiation, downward longwave radiation, specific humidity, pressure, wind speed, surface atmospheric CO_2 concentration, and atmospheric N and P deposition. In this study, the meteorological forcing variables were taken from 0.5° × 0.5° CRUNCEP version 5 (New et al., 1999, 2000, 2002) from 1901 to 2013 and interpolated into hourly for driving CABLE (Zhang et al., 2016). The atmospheric CO_2 concentration was the observed record over 1901–2010 (Keeling & Whorf, 2005), and the data of atmospheric N and P deposition rates we used in this study were from Hartmann et al. (2014). CABLE (without wind erosion process) was firstly spin-up from 1901 to 1910 forced by CRUNCEP data and an atmospheric CO_2 concentration of 296.64 ppm (e.g., 1901 level). A semianalytical solution method was used to accelerate the spin-up to steady state of coupled C-N-P processes in CABLE (Xia et al., 2012). Then, we ran CABLE (without wind erosion process) over 1901 to 1979 to provide a restart file at 1980 for our experiment in this study. Finally, we conducted the control simulation (CABLE without wind erosion) and the treatment simulation (CABLE with wind erosion) over 1980 to 2013. The treatment simulation has outputs of direct SOC loss by wind (C_{loss}-based field experiment equation with environment factors, see equation (10)), N_{loss} (equation (2)), Nm_{loss} (equation (3)), and annual total C_{pool} and N_{pool}.

The simulated absolute effect of wind erosion on C or N pool in CABLE model was calculated as

$$\text{Absolute effect} = \text{Treatment} - \text{Control} \tag{9}$$

where the Control and Treatment represented the simulations under the control and wind erosion scenarios, respectively. Thus, the reduction of C or N pool associated with wind erosion was defined as a negative value and the increase of C or N pool associated with wind erosion was defined as a positive value in the CABLE model. The simulated indirect SOC change was calculated by the difference between total SOC change and direct SOC loss.

3. Results

3.1. The Temporal and Spatial Patterns of Observed SOC Losses by Wind Erosion

The observed SOC losses under the wind erosion treatment with 25 m/s wind speed were different between the spring and autumn of 2014 (Figures 2a and 2b). The averaged SOC loss in spring (66.91 mg $C{\cdot}m^{-2}{\cdot}s^{-1}$) was larger than that in autumn (22.90 mg $C{\cdot}m^{-2}{\cdot}s^{-1}$). The observed SOC losses were highly variable from east to west with a range from 1.69 to 452.91 mg $C{\cdot}m^{-2}{\cdot}s^{-1}$ in the spring of 2014 (Figure 2a). In the autumn of 2014, SOC losses varied from 1.57 to 127.23 mg $C{\cdot}m^{-2}{\cdot}s^{-1}$ (Figure 2b). Higher SOC losses (>50 mg $C{\cdot}m^{-2}{\cdot}s^{-1}$) under the wind erosion treatment were detected in southwestern Inner Mongolia in the autumn of 2014. Greater SOC losses (>50 mg $C{\cdot}m^{-2}{\cdot}s^{-1}$) were mainly observed in western Inner Mongolia (Ala Shan Desert) and Gansu in 2015 and 2016 (Figure 2c). Across the 2 years, SOC losses were, on average, 29.11 mg $C{\cdot}m^{-2}{\cdot}s^{-1}$, varying from 0.01 to 375.83 mg $C{\cdot}m^{-2}{\cdot}s^{-1}$. The averaged SOC loss was 14.19 mg $C{\cdot}m^{-2}{\cdot}s^{-1}$ in 2015 and 36.29 mg $C{\cdot}m^{-2}{\cdot}s^{-1}$ in 2016.

3.2. Relationships of SOC Losses With Environmental Factors

Using the field measurements, we analyzed how SOC losses varied with different environmental factors, particularly wind speed and SWC in the semiarid or arid regions. We used square of wind speed (U^2) instead of wind speed because U^2 represents the linear relationship of the magnitude of wind power onto the mass of soil on the ground. Our data showed that the observed SOC losses increased with increasing U^2 in the spring of 2014 (Figure 3a). The averaged SOC losses were 9.82, 36.38, 47.33, and 66.91 mg $C{\cdot}m^{-2}{\cdot}s^{-1}$ under U^2 of 144, 256, 441, and 625 m^2/s^2, respectively.

To evaluate the relationship of SOC losses with SWC, we averaged the measured SOC losses under the same SWC (accurate to 1 $V/V\%$) with 25-m/s wind speed from 2014 to 2016. Observed SOC losses showed nonlinear response to SWC (Figure 3b). With increasing SWC (mean ± SE) from 0.52 to 25.44 $V/V\%$, SOC losses decreased from 38.54 to 5.86 mg $C{\cdot}m^{-2}{\cdot}s^{-1}$. The highest and lowest values of the observed SOC losses were 46.62 ± 22.76 and 1.52 ± 0.85 mg $C{\cdot}m^{-2}{\cdot}s^{-1}$ with the 5.52 ± 0.07 and 14.38 ± 0.08 $V/V\%$ SWC, respectively.

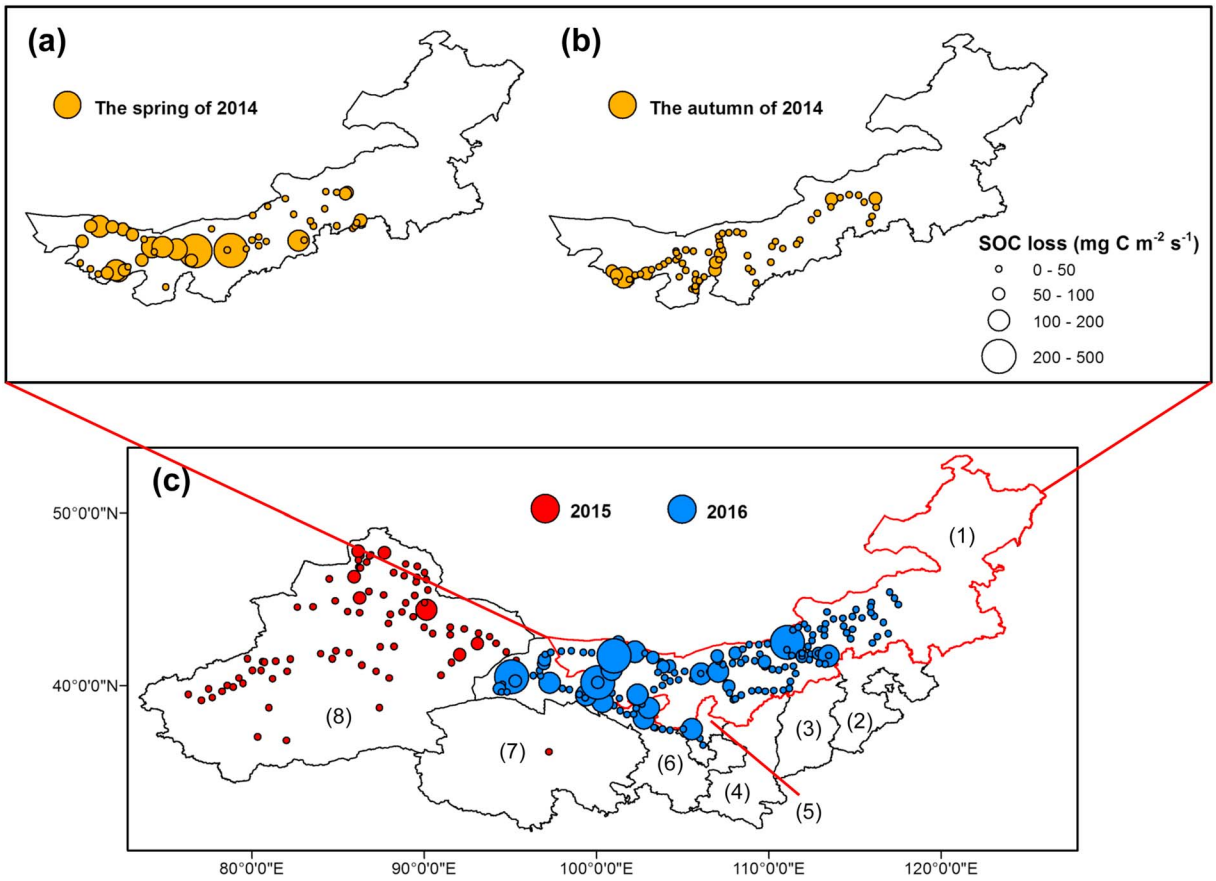

Figure 2. Observed soil organic carbon (SOC) losses under the wind erosion treatment with 25-m/s wind speed in Inner Mongolia in the (a) spring and (b) autumn of 2014 and (c) in northwest China in the spring of 2015 and 2016. (1) Inner Mongolia, (2) Hebei, (3) Shanxi, (4) Shaanxi, (5) Ningxia, (6) Gansu, (7) Qinghai, and (8) Xinjiang.

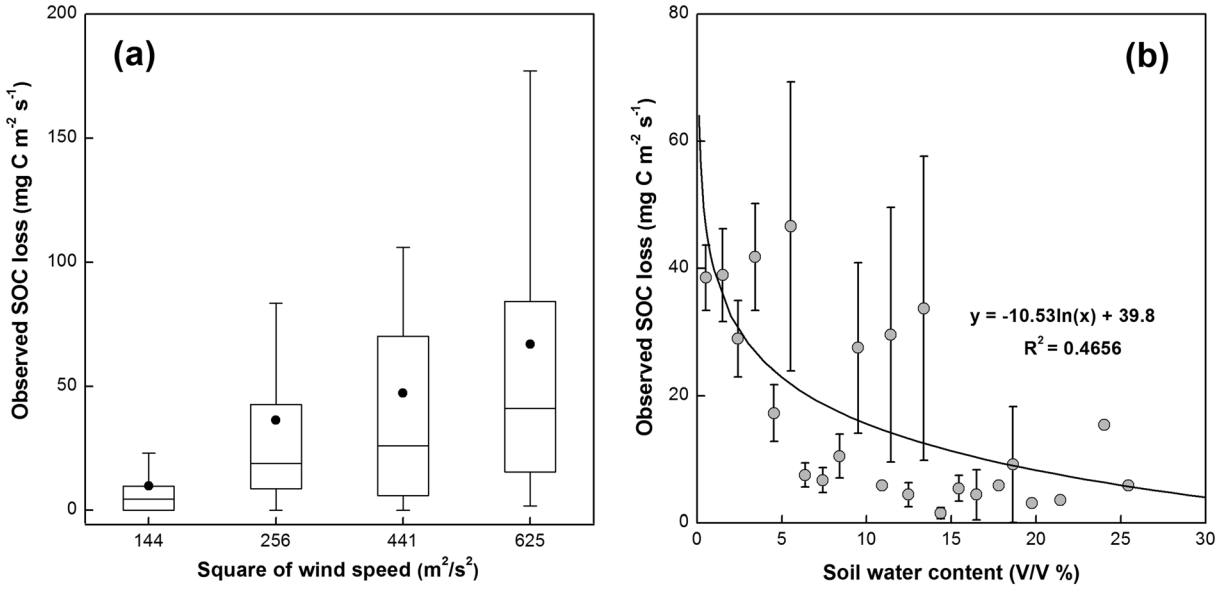

Figure 3. (a) The relationship of observed soil organic carbon (SOC) losses with the square of wind speed in the spring of 2014 in Inner Mongolia. The black circles are the averaged SOC losses under the four wind speed treatments. (b) The relationship of observed SOC losses (mean ± standard error) with soil water content under the wind erosion treatment with 25-m/s wind speed from 2014 to 2016.

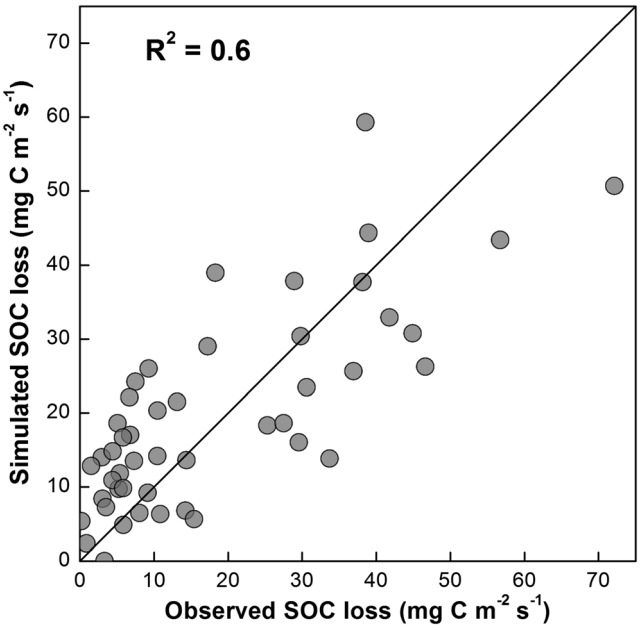

Figure 4. Relationship between simulated soil organic carbon (SOC) loss and observed SOC loss. The black line is 1:1 line.

Based on the observed relationships of SOC loss (g C) with wind speed (m/s) and SWC (V/V), we fit the following empirical model:

$$C_{loss} = a \times U^2 + b \times \ln(SWC) + c \quad (10)$$

where a, b, and c were parameters that were estimated as 0.0000395, −0.014, and −0.039, respectively, from the observed data in this study. To evaluate the performance of the empirical relationship (equation (10)), we compared simulated SOC loss using equation (10) with the observed SOC losses. The simulated SOC losses matched well with the observed data ($R^2 = 0.6$; Figure 4). The relationships of SOC loss caused by wind erosion with environmental factors were assumed to have no change from 1980 to 2013. This empirical relationship was used in CABLE for quantifying the effect of wind erosion on SOC loss in the study region.

3.3. Spatial Patterns of Total SOC Losses and Contributions of Direct and Indirect SOC Losses

Across the period from 1980 to 2013, the simulated total cumulative change in SOC pool in northwest China associated with wind erosion included direct SOC change and indirect SOC change using the CABLE model (Figure 5). In this region, the total cumulative change in SOC pool ranged from an increase of 0.25 g C/m^2 to a reduction of 152.33 g C/m^2 (Figure 5a). Greater intensity of SOC losses (>10 g C/m^2) occurred in eastern Ningxia, western Inner Mongolia, and central Xinjiang than other areas. The direct effect of wind erosion reduced SOC pool across all the areas in this region, with the largest cumulative SOC loss of 126.44 g C/m^2 over the 34 years in a certain area (Figure 5b). The indirect effect of wind erosion on SOC pool in northwest China ranged from −32.56 to 9.96 g C/m^2 over the 34 years (Figure 5c). The SOC pool induced by the indirect effect of wind erosion increased (>1 g C/m^2) in eastern Ningxia but reduced (< −1 g C/m^2) in central Xinjiang. Indirect cumulative SOC change offsets direct cumulative SOC loss, leading to an increase in SOC storage in some areas, such as central of Inner Mongolia (Figure 5a).

3.4. Interannual Variations of Ecosystem C and Soil N Pools and SOC Losses

The cumulative losses in plant C pool, SOC pool, and soil N pool caused by wind erosion all showed increasing trends in northwest China from 1980 to 2013 (Figures 6a and 6b). Litter C pool was enhanced by wind erosion during the first 9 years in the 1980s, with the largest increase of 0.82 Tg C in 1984, but was reduced from 1989 to 2013 (Figure 6a). The enhanced litter C pool in the 1980s could be ascribed to the decrease in decomposition rate associated with N limitation (equations (7) and (8)). The declining trend of litter C pool after 1984 might be caused by the reduced input from plant biomass. By 1989, the total litter C pool fell below the initial pool size in 1980.

The maximum and minimum of annual direct SOC losses were 0.87 Tg C/year in 1980 and 0.61 Tg C/year in 2013, respectively (Figure 6c). SOC pool was rapidly reduced from 1981 to 1983 due to indirect effect of wind erosion (Figure 6d). By contrast, indirect effect of wind erosion led to an increase in SOC accumulation over the next 5 years with the highest value in 1985 (0.04 Tg C/year). After 1988, the contribution of indirect effect of wind erosion to total SOC loss was intensified with time until 1997 when the largest reduction of 0.14 Tg C/year was detected. After that, the indirect SOC losses were generally alleviated over time.

3.5. Spatial Patterns of Wind Erosion Effect on C Fluxes

Over the 34 years, changes of mean annual NPP by wind erosion ranged from −5.57 to 0.08 g C·m^{-2}·year^{-1} in northwest China (Figure 7a). Greater reduction of NPP (>1 g C·m^{-2}·year^{-1}) mainly occurred in western Inner Mongolia and central Xinjiang. Mean annual R_h was declined in western Inner Mongolia and central Xinjiang, with the largest reduction of 3.92 g C·m^{-2}·year^{-1} (Figure 7b). Thus, changes of mean annual net ecosystem productivity caused by wind erosion showed a large spatial variation in northwest China over the 34 years (Figure 7c). Mean annual net ecosystem productivity was increased (>0.1 g C·m^{-2}·year^{-1}) in

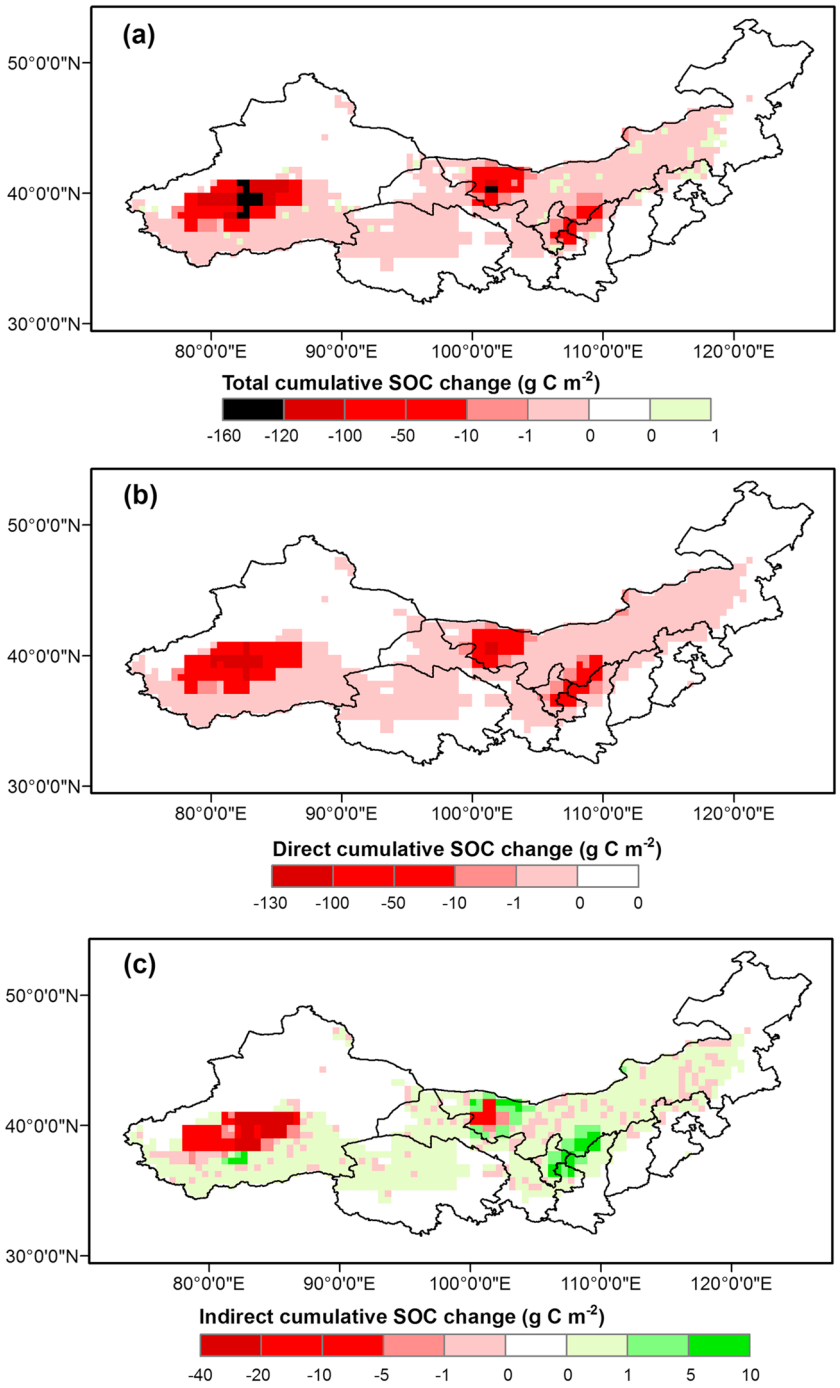

Figure 5. Spatial patterns of (a) total, (b) direct, and (c) indirect cumulative soil organic carbon (SOC) change associated with wind erosion in northwest China over the time period from 1980 to 2013.

eastern Ningxia but reduced (< -0.1 g C·m^{-2}·year^{-1}) in central Xinjiang by wind erosion, which was consistent with that of indirect cumulative SOC change.

3.6. The Effect of Wind Erosion on Different Components of Ecosystem C and N Pools

Over the 34 years, wind erosion directly reduced soil C and N pools by 24.79 Tg C and 1.52 Tg N, respectively, in northwest China (Figure 8). The CABLE model used in this study, for the first time, considered the feedback of soil N loss to plant productivity as well as plant and soil C pools. Results showed that soil N loss

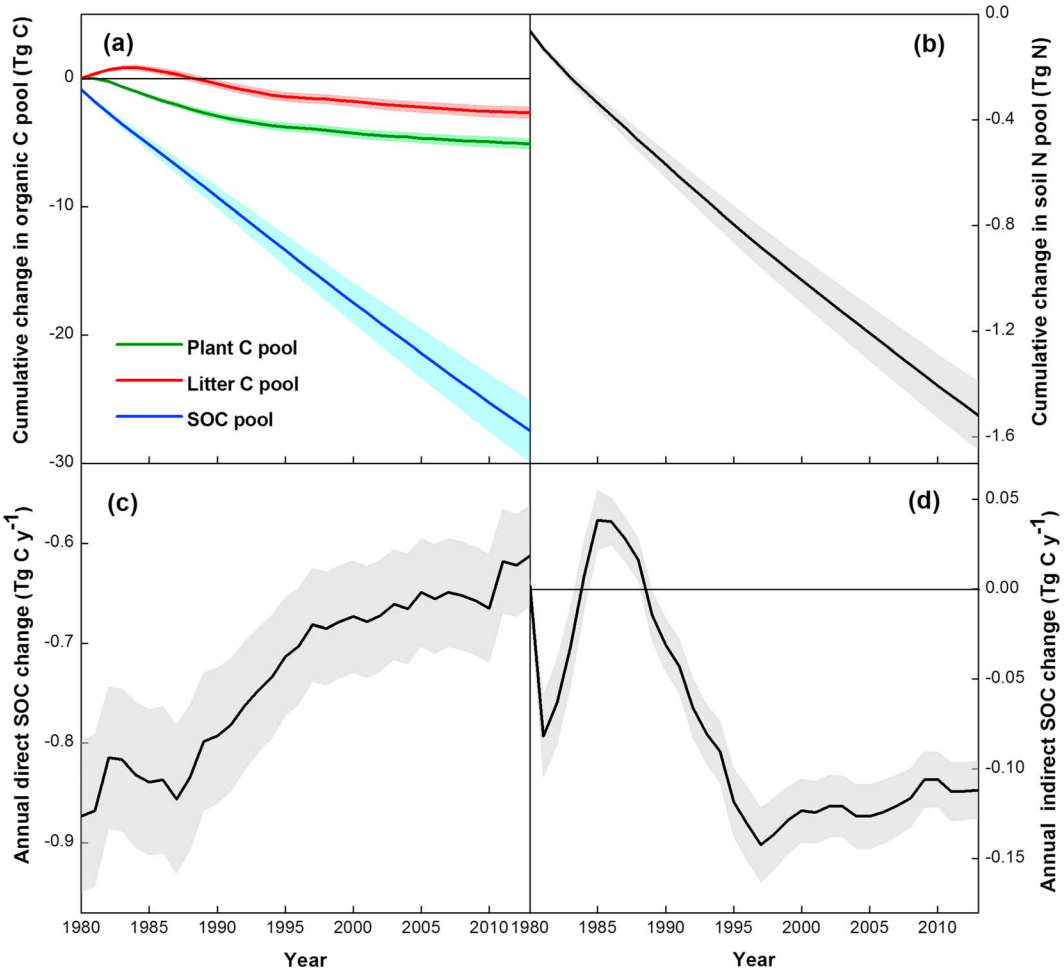

Figure 6. Simulated cumulative changes in (a) plant C pool, litter C pool, soil organic carbon (SOC) pool, and (b) soil N pool associated with wind erosion in northwest China from 1980 to 2013. Annual dynamics of SOC pool change induced by (c) direct and (d) indirect effects of wind erosion in northwest China over the 34 years. The shaded areas represent the standard error of simulations in this area.

associated with wind erosion reduced NPP (Figure 7), leading to decreased plant C pool (5.13 Tg C) and subsequent litter C pool (2.67 Tg C). Given the reductions of C input from plants to soil (e.g., NPP) and C output from soil (e.g., R_h), SOC storage was indirectly decreased by 2.68 Tg C over the 34 years. Thus, the total reduction of SOC storage in northwest China associated with wind erosion was 27.47 Tg C over the 34 years.

4. Discussion

4.1. The Relationships of Direct SOC Losses With Environmental Factors

Several previous studies focused on the relationship of direct SOC loss caused by wind erosion with environmental factors in laboratory or site-scale experiments (Dong et al., 2002; Maurer et al., 2006; Xue et al., 2011), but the results are difficult to be extrapolated to the regional scales. In this study, we conducted a large-scale field survey in the arid and semiarid regions of northwest China, covering more than 3,500 km from east to west (Figure 1). Previous studies have demonstrated that wind speed and soil water content are important environmental factors affecting SOC loss caused by wind erosion (Chen et al., 1996; Dong et al., 2003). Our results also showed that SOC loss associated with wind erosion positively depended upon wind speed and was negatively related with soil water content (Figure 3). The variations of SOC loss with wind speed have been demonstrated by many experimental studies (Gomes et al., 2003; Munson et al., 2011). Since kinetic energy is positively correlated with the square of velocity, wind erosion rate increases with wind speed (Dong et al., 2003). In arid and semiarid regions, soil water content is an important resistance factor

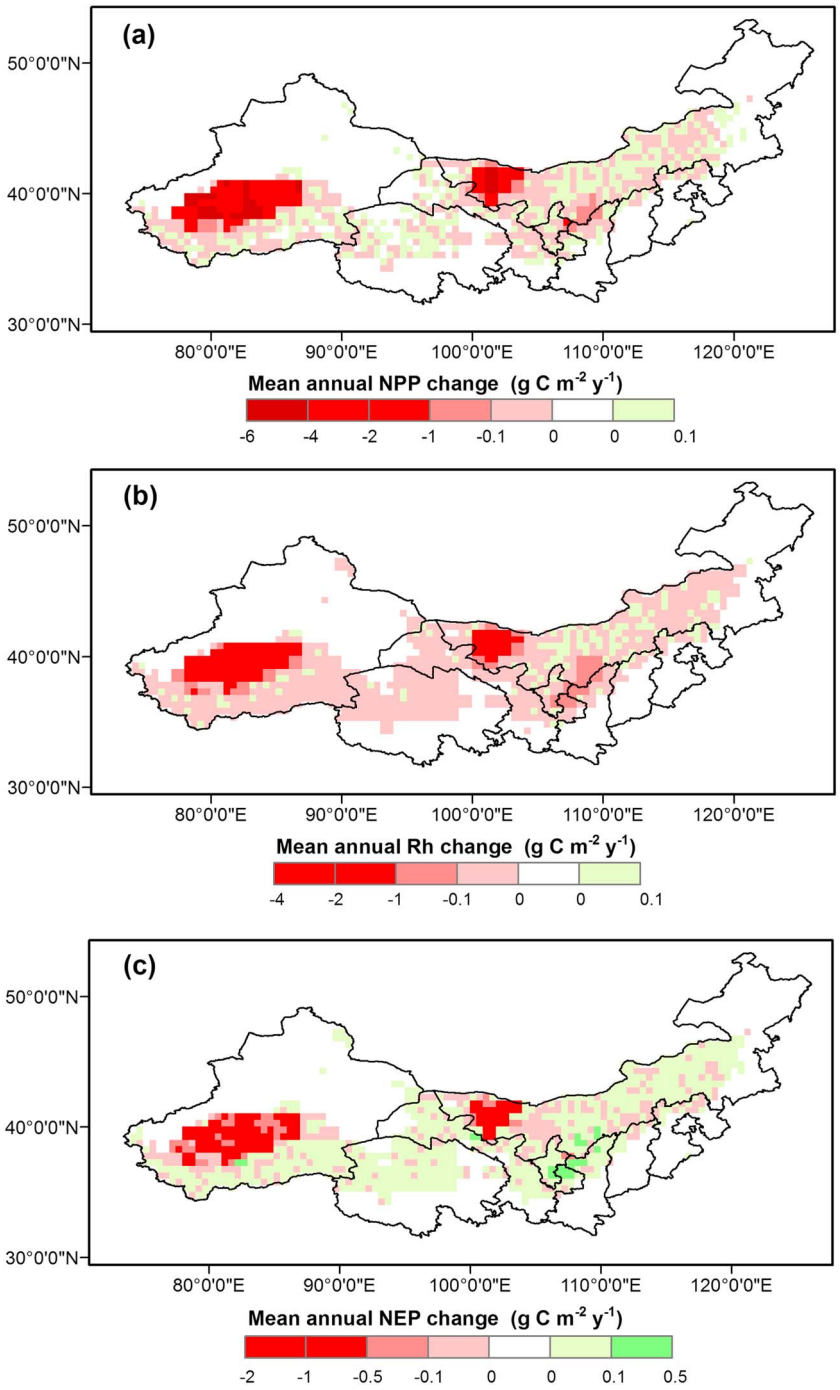

Figure 7. Spatial patterns of wind erosion effect on mean annual (a) net primary productivity (NPP), (b) heterotrophic respiration (Rh), and (c) net ecosystem productivity (NEP) in northwest China over the time period from 1980 to 2013.

that influences the magnitude of SOC loss associated with wind erosion (Chen et al., 1996; Dong et al., 2002). Lower soil water content leads to a reduction of cohesive force (Chen et al., 1996), and thus dry soil is more likely to be blown away by the wind (Yan et al., 2002). The lower observed SOC losses in the autumn than spring of 2014 (Figures 2a and 2b) could be attributed to the greater soil water content in the autumn (Figure S2) due to that the majority of precipitation occurs in May to October in the arid and semiarid regions (Feng et al., 2016; Lei et al., 2018). Due to the larger SOC loss associated with wind erosion in spring, most field surveys in this study were conducted in the spring of 2014–2016.

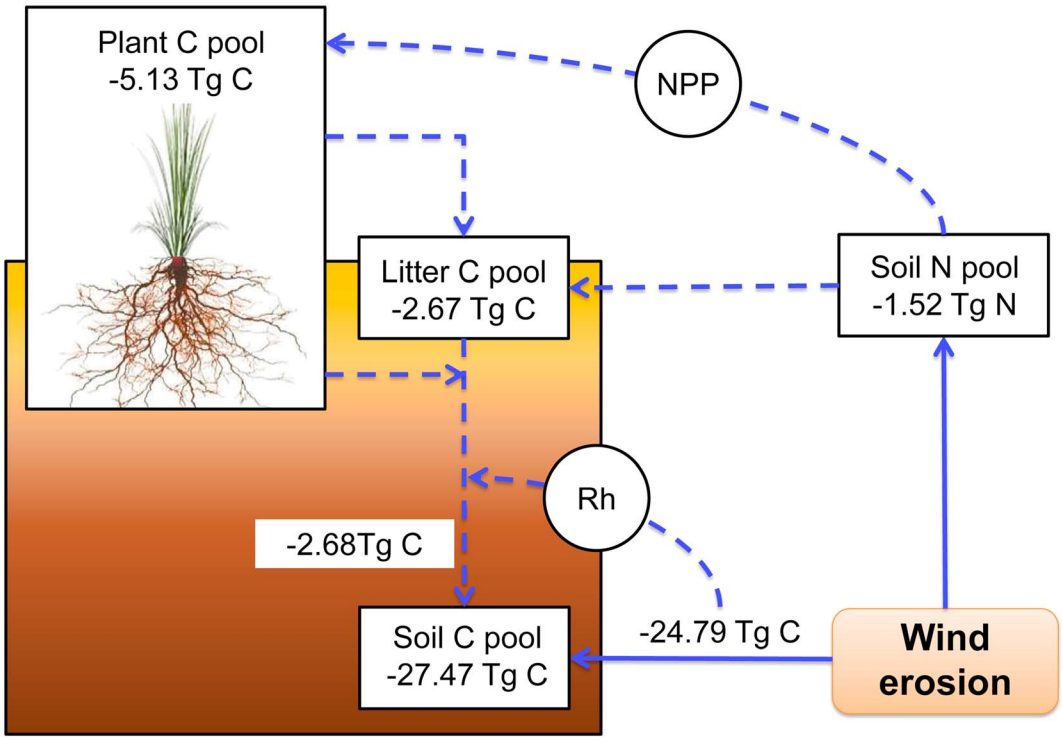

Figure 8. Diagram of direct and indirect effects of wind erosion on ecosystem carbon (C) and soil nitrogen (N) pools. The negative values show C or N losses. The solid and dash lines represent the direct and indirect effects of wind erosion on ecosystem C or N pools, respectively. NPP = net primary productivity.

4.2. The Direct Effect of Wind Erosion on SOC Storage

Greater SOC losses in eastern Ningxia, western Inner Mongolia, and central Xinjiang (Figure 5b) directly caused by wind erosion simulated by the CABLE model in this study is in agreement with the potential dust source regions by Shao et al. (2011). The simulated dust emission (401.10 Tg soil/year) of Song et al. (2016) and SOC loss (75 Tg C/year) of Yan et al. (2005) are both larger than the direct SOC loss (0.73 Tg C/year) in the CABLE model in this study. This lower SOC loss is because the percentage content of sand is fixed and soil particle smaller than 20 μm in diameter is selectively removed by wind erosion (equation (1)), which is fitted with the observed soil particle diameter in dust emission (Chen & Fryrear, 2002). The attenuation of annual direct SOC loss (Figure 6c) could be ascribed to the reduction of fine particle content in soil surface (equation (1); Xue et al., 2011). Although the empirical model (equation (10)) can fit well the field observations (Figure 4), it has been reported that soil loss by wind erosion could be also affected by other variables, such as soil texture (Calzo & Buschiazzo, 2010; Zamani & Mahmoodabadi, 2013), surface roughness (Hagen, 2008; Visser et al., 2004), and climate change (Xue et al., 2011). Therefore, accurate assessments on the effects of environmental factors on direct SOC loss in large-scale experiments are necessary to better predict SOC storage under the wind erosion scenario.

4.3. The Indirect Effect of Wind Erosion on SOC Storage

Great research efforts have been devoted to the impacts of wind erosion on soil C storage at regional and global scales (Borrelli et al., 2017; Shao et al., 2011; Yan et al., 2005). Nevertheless, the indirect effect of wind erosion on soil C pool through removing soil N and thus suppressing plant productivity and C input have never been explored. In this study, data of SOC loss derived from the field investigation and sampling were used to parameterize the CABLE model and then simulated the indirect effects of wind erosion over the time period from 1980 to 2013. At the regional scale, the 9.76% contributions of indirect effect of wind erosion to total SOC loss in northwest China (Figure 5) suggest that SOC storage would be overestimated if we neglect plant productivity feedback to SOC pools under the wind erosion scenario. The enhanced SOC storage by indirect effect of wind erosion in eastern Ningxia (Figure 5c) is attributed to the reduction

of C output from soil (Figure 7b). Though decreased R_h offsets NPP loss resulting in the increase of SOC storage in some areas, indirect ecosystem C loss was aggravated with the increase of direct cumulative SOC loss associated with wind erosion (Figure S3).

Over the 34 years, due to the N limitation on litter decomposition rate (equations (7) and (8)), litter C pool increased in the first 9 years (Figure 6a). Decreased C output from soil offset the reduction of C input from litter to soil, leading to the increase of SOC storage from 1984 to 1988 (Figure 6d). However, when soil N loss is intensified with time by wind erosion (Figure 6b; Li et al., 2004), plant growth is restricted by lowered soil N availability (Luo et al., 2004; Thomas et al., 2015). Reduced soil N availability leads to suppression of leaf area, leaf photosynthesis, and leaf-N content (Zhao et al., 2005). The changes of leaf area and photosynthetic capacity directly influence plant productivity (Sinclair, 1990). Reductions of NPP by wind erosion (Figure 7a; Gantzer et al., 1990; Lal, 1995) aggravated indirect SOC loss through decreasing organic C input from litter to soil. Consequently, the decrease of annual NPP (Figure 7a) results in the enhanced SOC loss after 1988 (Figure 6d). The negative feedback of plant productivity exacerbates on SOC losses associated with wind and leads to greater reductions of SOC pool.

4.4. The Challenges and Significance of Assessing Wind Erosion Effect on SOC Storage

Quantification of SOC losses by wind erosion is critical for evaluating SOC storage in arid and semiarid regions (Borrelli et al., 2017; Tian et al., 2015). The two commonly used approaches include the tracer method and the wind tunnel. The tracer method uses isotope such as cesium-137 (^{137}Cs) to estimate soil redistribution with a soil erosion model (Ritchie & McHen, 1990). This method has been used in Australia (Chappell et al., 2012) where it shows that soil erosion is reduced by soil conservation measures. However, larger uncertainty of measurements (e.g., the measurement error of the reference ^{137}Cs level) often leads to substantial spatial variability (Chappell et al., 2012; Li et al., 2010). The wind tunnel simulates the wind effect on soil surface (Maurer et al., 2006; Zhang et al., 2004) but has difficulty in simulating wind erosion under natural surface conditions across vast regions with various vegetation type, topography soil type, precipitation, and soil moisture conditions (Maurer et al., 2006). Ecosystem models have also been used to simulate the effect of wind erosion on soil C cycling at regional or global scales (Borrelli et al., 2017; Song et al., 2016). However, Wu et al. (2018) simulated wind erosion in East Asia using 15 climate models and found that models cannot reproduce the observed wind erosion event frequency. In this study, we used a new approach to simulate natural wind erosion, which avoided measuring the error caused by changing experimental conditions. This new approach can provide critical model parameterizations to assess soil C losses at regional scales.

Another advantage of this study was incorporating the wind erosion process into the process-based, coupled C-N ecosystem model (e.g., CABLE model) and providing a novel platform to simulate the wind erosion effect on SOC storage in northwest China. In addition to simulating direct SOC loss by wind erosion, the improved CABLE model simulated the indirect effect of wind erosion on SOC storage through feedback of suppressed plant productivity. However, the improved CABLE model in this study is only applicable in dust emission source areas, such as northwest China. It is necessary to incorporate a dust transport submodel with CABLE in the future to simulate larger spatial scales. In summary, the indirect effect of wind erosion aggravates soil C losses in the northwest China, highlighting the importance of plant feedback to SOC storage changes associated with wind erosion.

5. Conclusions

This study demonstrated that wind erosion not only influenced SOC storage through directly removing land surface soil but also indirectly affected SOC storage via feedback of suppressed plant productivity. This work, for the first time, quantified the indirect effect of wind erosion on SOC storage caused by feedback of decreased plant productivity. Soil N loss associated with wind erosion decreased NPP, causing reductions of plant C pool and subsequent litter C pool. Given the decreased organic C input from plant C pool to soil C pool, SOC storage in northwest China was indirectly decreased by 2.68 Tg C from 1980 to 2013, which contributed to 9.76% of the total SOC losses. Omitting plant feedback could underestimate wind erosion effect on SOC storage. Therefore, plant feedback should be considered in the ecosystem models to accurately evaluate SOC storage associated with wind erosion at the regional or global scales.

Acknowledgments

We thank Congcong Wang, Jie Chen, Dan Yang, Shizheng Men, Huiling Liu, Qiao Jiang, Qingxia Yang, and Yun Guo for help in laboratory. This project was financially supported by the National Natural Science Foundation of China (31430015). The simulated data for this paper have been deposited in a general repository (https://figshare.com/s/e0754329808dcfa69c97). The observed data of the large-scale field experiment can be obtained by contacting the corresponding author S. Wan (swan@ib-cas.ac.cn).

References

Batjes, N. H. (1996). Total carbon and nitrogen in the soils of the world. *European Journal of Soil Science*, *47*(2), 151–163. https://doi.org/10.1111/j.1365-2389.1996.tb01386.x

Best, M. J., Abramowitz, G., Johnson, H. R., Pitman, A. J., Balsamo, G., Boone, A., et al. (2015). The plumbing of land surface models: Benchmarking model performance. *Journal of Hydrometeorology*, *16*(3), 1425–1442. https://doi.org/10.1175/JHM-D-14-0158.1

Borrelli, P., Lugato, E., Montanarella, L., & Panagos, P. (2017). A new assessment of soil loss due to wind erosion in European agricultural soils using a quantitative spatially distributed modelling approach. *Land Degradation and Development*, *28*(1), 335–344. https://doi.org/10.1002/ldr.2588

Bremer, E., & Kuikman, P. (1994). Microbial utilization of ^{14}C[U]glucose in soil is affected by the amount and timing of glucose additions. *Soil Biology and Biochemistry*, *26*(4), 511–517. https://doi.org/10.1016/0038-0717(94)90184-8

Calzo, J. C., & Buschiazzo, D. E. (2010). Soil dry aggregate stability and wind erodible fraction in a semiarid environment of Argentina. *Geoderma*, *159*(1–2), 228–236. https://doi.org/10.1016/j.geoderma.2010.07.016

Chappell, A., Baldock, J., & Sanderman, J. (2016). The global significance of omitting soil erosion from soil organic carbon cycling schemes. *Nature Climate Change*, *6*(2), 187–191. https://doi.org/10.1038/nclimate2829

Chappell, A., Sanderman, J., Thomas, M., Read, A., & Leslie, C. (2012). The dynamics of soil redistribution and the implications for soil organic carbon accounting in agricultural south-eastern Australia. *Global Change Biology*, *18*(6), 2081–2088. https://doi.org/10.1111/j.1365-2486.2012.02682.x

Chen, W., Dong, Z., Li, Z., & Yang, Z. (1996). Wind tunnel test of the influence of moisture on the erodibility of loessial sandy loam soils by wind. *Journal of Arid Environments*, *34*(4), 391–402. https://doi.org/10.1006/jare.1996.0119

Chen, W., & Fryrear, D. W. (2002). Sedimentary characteristics of a haboob dust storm. *Atmospheric Research*, *61*(1), 75–85. https://doi.org/10.1016/S0169-8095(01)00092-8

De Kauwe, M. G., Medlyn, B. E., Walker, A. P., Zaehle, S., Asao, S., Guenet, B., et al. (2017). Challenging terrestrial biosphere models with data from the long-term multifactor prairie heating and CO_2 enrichment experiment. *Global Change Biology*, *23*(9), 3623–3645. https://doi.org/10.1111/gcb.13643

Dong, Z., Liu, X., Wang, H., & Wang, X. (2003). Aeolian sand transport: A wind tunnel model. *Sedimentary Geology*, *161*(1–2), 71–83. https://doi.org/10.1016/S0037-0738(02)00396-2

Dong, Z., Liu, X., & Wang, X. (2002). Wind initiation thresholds of the moistened sands. *Geophysical Research Letters*, *29*(12), 1585. https://doi.org/10.1029/2001GL013128

Feng, J., Turner, B. L., Lü, X., Chen, Z., Wei, K., Tian, J., et al. (2016). Phosphorus transformations along a large-scale climosequence in arid and semiarid grasslands of northern China. *Global Biogeochemical Cycles*, *30*, 1264–1275. https://doi.org/10.1002/2015GB005331

Fontaine, S., Barot, S., Barré, P., Bdioui, N., Mary, B., & Rumpel, C. (2007). Stability of organic carbon in deep soil layers controlled by fresh carbon supply. *Nature*, *450*(7167), 277–280. https://doi.org/10.1038/nature06275

Gantzer, C. J., Anderson, S. H., Thompson, A. L., & Brown, J. R. (1990). Estimating soil erosion after 100 years of cropping on Sanborn Field. *Journal of Soil and Water Conservation*, *45*(6), 641–644.

Gomes, L., Arrue, J. L., Lopez, M. V., Sterk, G., Richard, D., Gracia, R., et al. (2003). Wind erosion in a semiarid agricultural area of Spain the WELSONS project. *Catena*, *52*(3–4), 235–256. https://doi.org/10.1016/S0341-8162(03)00016-X

Gregorich, G. E., Greer, K. J., Anderson, D. W., & Liang, B. C. (1998). Carbon distribution and losses: Erosion and deposition effects. *Soil and Tillage Research*, *47*(3–4), 291–302. https://doi.org/10.1016/S0167-1987(98)00117-2

Hagen, L. J. (2002). Processes of soil erosion by wind. *Annals of Arid Zone*, *40*(3), 235–254.

Hagen, L. J. (2008). Updating soil surface conditions during wind erosion events using the Wind Erosion Prediction System (WEPS). *Transactions of the ASABE*, *51*(1), 129–137. https://doi.org/10.13031/2013.24233

Hartmann, J., Moosdorf, N., Lauerwald, R., Hinderer, M., & West, A. J. (2014). Global chemical weathering and associated P-release—The role of lithology, temperature and soil properties. *Chemical Geology*, *363*, 145–163. https://doi.org/10.1016/j.chemgeo.2013.10.025

Kattge, J., Knorr, W., Raddatz, T., & Wirth, C. (2009). Quantifying photosynthetic capacity and its relationship to leaf nitrogen content for global-scale terrestrial biosphere models. *Global Change Biology*, *15*(4), 976–991. https://doi.org/10.1111/j.1365-2486.2008.01744.x

Keeling, C. D., & Whorf, T. P. (2005). Atmospheric CO_2 records from sites in the SIO air sampling network, trends: A compendium of data on global change. Oak Ridge, TN: Oak Ridge National Laboratory, US Department of Energy, USA: Carbon Dioxide Information Analysis Center.

Kok, J. F. (2011). A scaling theory for the size distribution of emitted dust aerosols suggests climate models underestimate the size of the global dust cycle. *Proceedings of the National Academy of Sciences*, *108*(3), 1016–1021. https://doi.org/10.1073/pnas.1014798108

Lal, R. (1995). Erosion-crop productivity relationships for soils of Africa. *Soil Science Society of America Journal*, *59*(3), 661–667. https://doi.org/10.2136/sssaj1995.03615995005900030004x

Lal, R. (2003). Soil erosion and the global carbon budget. *Environment International*, *29*(4), 437–450. https://doi.org/10.1016/S0160-4120(02)00192-7

LeBauer, D. S., & Treseder, K. K. (2008). Nitrogen limitation of net primary productivity in terrestrial ecosystems is globally distributed. *Ecology*, *89*(2), 371–379. https://doi.org/10.1890/06-2057.1

Leff, J. W., Wieder, W. R., Taylor, P. G., Townsend, A. R., Nemergut, D. R., Grandy, A. S., & Cleveland, C. C. (2012). Experimental litterfall manipulation drives large and rapid changes in soil carbon cycling in a wet tropical forest. *Global Change Biology*, *18*(9), 2969–2979. https://doi.org/10.1111/j.1365-2486.2012.02749.x

Lei, L., Xia, J., Li, X., Huang, K., Zhang, A., Chen, S., et al. (2018). Water response of ecosystem respiration regulates future projection of net ecosystem productivity in a semiarid grassland. *Agricultural and Forest Meteorology*, *252*, 175–191. https://doi.org/10.1016/j.agrformet.2018.01.020

Li, F., Zhao, L., Zhang, H., Zhang, T., & Shirato, Y. (2004). Wind erosion and airborne dust deposition in farmland during spring in the Horqin Sandy Land of eastern Inner Mongolia, China. *Soil and Tillage Research*, *75*(2), 121–130. https://doi.org/10.1016/j.still.2003.08.001

Li, P., Liu, L., Wang, J., Wang, Z., Wang, X., Bai, Y., & Chen, S. (2018). Wind erosion enhanced by land use changes significantly reduces ecosystem carbon storage and carbon sequestration potentials in semiarid grasslands. *Land Degradation and Development*, *29*(10), 3469–3478. https://doi.org/10.1002/ldr.3118

Li, S., Lobb, D. A., Tiessen, K. H., & McConkey, B. G. (2010). Selecting and applying cesium-137 conversion models to estimate soil erosion rates in cultivated fields. *Journal of Environmental Quality*, *39*(1), 204–219. https://doi.org/10.2134/jeq2009.0144

Liu, L., King, J., Booker, F. L., Giardina, C. P., Allen, H. L., & Hu, S. (2009). Enhanced litter input rather than changes in litter chemistry drive soil carbon and nitrogen cycles under elevated CO_2: A microcosm study. *Global Change Biology*, *15*(2), 441–453. https://doi.org/10.1111/j.1365-2486.2008.01747.x

Lu, M., Zhou, X., Luo, Y., Yang, Y., Fang, C., Chen, J., & Li, B. (2011). Minor stimulation of soil carbon storage by nitrogen addition: A meta-analysis. *Agriculture, Ecosystems and Environment*, *140*(1–2), 234–244. https://doi.org/10.1016/j.agee.2010.12.010

Luo, Y., Su, B. O., Currie, W. S., Dukes, J. S., Finzi, A., Hartwig, U., et al. (2004). Progressive nitrogen limitation of ecosystem responses to rising atmospheric carbon dioxide. *Bioscience*, *54*(8), 731–739. https://doi.org/10.1641/0006-3568(2004)054[0731:PNLOER]2.0.CO;2

Maurer, T., Herrmann, L., Gaiser, T., Mounkaila, M., & Stahr, K. (2006). A mobile wind tunnel for wind erosion field measurements. *Journal of Arid Environments*, *66*(2), 257–271. https://doi.org/10.1016/j.jaridenv.2005.11.002

Munson, S. M., Belnapa, J., & Okin, G. S. (2011). Responses of wind erosion to climate-induced vegetation changes on the Colorado plateau. *Proceedings of the National Academy of Sciences*, *108*(10), 3854–3859. https://doi.org/10.1073/pnas.1014947108

New, M., Hulme, M., & Jones, P. (1999). Representing twentieth-century space-time climate variability. Part I: Development of a 1961–90 mean monthly terrestrial climatology. *Journal of Climate*, *12*(3), 829–856. https://doi.org/10.1175/1520-0442(1999)012<0829:RTCSTC>2.0.CO;2

New, M., Hulme, M., & Jones, P. (2000). Representing twentieth-century space-time climate variability. Part II: Development of 1901–96 monthly grids of terrestrial surface climate. *Journal of Climate*, *13*(13), 2217–2238. https://doi.org/10.1175/1520-0442(2000)013<2217:RTCSTC>2.0.CO;2

New, M., Lister, D., Hulme, M., & Makin, I. (2002). A high-resolution data set of surface climate over global land areas. *Climate Research*, *21*, 1–25. https://doi.org/10.3354/cr021001

Niu, S., Wu, M., Han, Y. I., Xia, J., Zhang, Z. H. E., Yang, H., & Wan, S. (2010). Nitrogen effects on net ecosystem carbon exchange in a temperate steppe. *Global Change Biology*, *16*(1), 144–155. https://doi.org/10.1111/j.1365-2486.2009.01894.x

Niu, S., Xing, X., Zhang, Z., Xia, J., Zhou, X., Song, B., et al. (2011). Water-use efficiency in response to climate change: From leaf to ecosystem in a temperate steppe. *Global Change Biology*, *17*(2), 1073–1082. https://doi.org/10.1111/j.1365-2486.2010.02280.x

Piao, S., Yin, G., Tan, J., Cheng, L., Huang, M., Li, Y., et al. (2015). Detection and attribution of vegetation greening trend in China over the last 30 years. *Global Change Biology*, *21*(4), 1601–1609. https://doi.org/10.1111/gcb.12795

Ritchie, J. C., & McHen, J. R. (1990). Application of radioactive fallout cesium-137 for measuring soil erosion and sediment accumulation rates and patterns: A review. *Journal of Environmental Quality*, *19*(2), 215–233. https://doi.org/10.2134/jeq1990.00472425001900020006x

Shao, Y., Wyrwoll, K.-H., Chappell, A., Huang, J., Lin, Z., McTainsh, G. H., et al. (2011). Dust cycle: An emerging core theme in Earth system science. *Aeolian Research*, *2*(4), 181–204. https://doi.org/10.1016/j.aeolia.2011.02.001

Sinclair, T. R. (1990). Nitrogen influence on the physiology of crop yield. In R. Rabbinge, J. Goudriaan, H. van Keulen, F. W. T. Penning de Vries, & H. H. van Laar (Eds.), *Theoretical production ecology: Reflections and prospects* (pp. 41–45). Wageningen: Pudoc.

Song, H., Zhang, K., Piao, S., & Wan, S. (2016). Spatial and temporal variations of spring dust emissions in northern China over the last 30 years. *Atmospheric Environment*, *126*, 117–127. https://doi.org/10.1016/j.atmosenv.2015.11.052

Thomas, R. Q., Brookshire, E. N., & Gerber, S. (2015). Nitrogen limitation on land: How can it occur in earth system models? *Global Change Biology*, *21*(5), 1777–1793. https://doi.org/10.1111/gcb.12813

Tian, H., Lu, C., Yang, J., Banger, K., Huntzinger, D. N., Schwalm, C. R., et al. (2015). Global patterns and controls of soil organic carbon dynamics as simulated by multiple terrestrial biosphere models: Current status and future directions. *Global Biogeochemical Cycles*, *29*, 775–792. https://doi.org/10.1002/2014GB005021

Uno, I., Eguchi, K., Yumimoto, K., Takemura, T., Shimizu, A., Uematsu, M., et al. (2009). Asian dust transported one full circuit around the globe. *Nature Geoscience*, *2*(8), 557–560. https://doi.org/10.1038/ngeo583

Visser, S. M., Strek, G., & Ribolzi, O. (2004). Techniques for simultaneous quantification of wind and water erosion in semi-arid regions. *Journal of Arid Environments*, *59*(4), 699–717. https://doi.org/10.1016/j.jaridenv.2004.02.005

Wang, Y.-P., Houlton, B. Z., & Field, C. B. (2007). A model of biogeochemical cycles of carbon, nitrogen, and phosphorus including symbiotic nitrogen fixation and phosphatase production. *Global Biogeochemical Cycles*, *21*, GB1018. https://doi.org/10.1029/2006GB002797

Wang, Y.-P., Kowalczyk, E., Leuning, R., Abramowitz, G., Raupach, M. R., Pak, B., et al. (2011). Diagnosing errors in a land surface model (CABLE) in the time and frequency domains. *Journal of Geophysical Research*, *116*, G01034. https://doi.org/10.1029/2010JG001385

Wang, Y.-P., Law, R. M., & Pak, B. (2010). A global model of carbon, nitrogen and phosphorus cycles for the terrestrial biosphere. *Biogeosciences*, *7*(7), 2261–2282. https://doi.org/10.5194/bg-7-2261-2010

Wang, Y.-P., Lu, X. J., Wright, I. J., Dai, Y. J., Rayner, P. J., & Reich, P. B. (2012). Correlations among leaf traits provide a significant constraint on the estimate of global gross primary production. *Geophysical Research Letters*, *39*, L19405. https://doi.org/10.1029/2012GL053461

Webb, N. P., Chappell, A., Strong, C. L., Marx, S. K., & McTainsh, G. H. (2012). The significance of carbon-enriched dust for global carbon accounting. *Global Change Biology*, *18*(11), 3275–3278. https://doi.org/10.1111/j.1365-2486.2012.02780.x

Wu, C., Lin, Z., Liu, X., Li, Y., Lu, Z., & Wu, M. (2018). Can climate models reproduce the decadal change of dust aerosol in East Asia? *Geophysical Research Letters*, *45*, 9953–9962. https://doi.org/10.1029/2018GL079376

Xia, J., Luo, Y., Wang, Y.-P., Weng, E., & Hararuk, O. (2012). A semi-analytical solution to accelerate spin-up of a coupled carbon and nitrogen land model to steady state. *Geoscientific Model Development*, *5*(5), 1259–1271. https://doi.org/10.5194/gmd-5-1259-2012

Xia, J., Niu, S., & Wan, S. (2009). Response of ecosystem carbon exchange to warming and nitrogen addition during two hydrologically contrasting growing seasons in a temperate steppe. *Global Change Biology*, *15*(6), 1544–1556. https://doi.org/10.1111/j.1365-2486.2008.01807.x

Xia, J., & Wan, S. (2008). Global response patterns of terrestrial plant species to nitrogen addition. *New Phytologist*, *179*(2), 428–439. https://doi.org/10.1111/j.1469-8137.2008.02488.x

Xue, X., Luo, Y., Zhou, X., Sherry, R., & Jia, X. (2011). Climate warming increases soil erosion, carbon and nitrogen loss with biofuel feedstock harvest in tallgrass prairie. *GCB Bioenergy*, *3*(3), 198–207. https://doi.org/10.1111/j.1757-1707.2010.01071.x

Yan, H., Wang, C., & Niu, Z. (2002). Remote sensing estimation of wind erosion: Application to Asia dust. *Journal of soil and water conservation China*, *16*, 120–123.

Yan, H., Wang, S., Wang, C., Zhang, G., & Patel, N. (2005). Losses of soil organic carbon under wind erosion in China. *Global Change Biology*, *11*(5), 828–840. https://doi.org/10.1111/j.1365-2486.2005.00950.x

Zaehle, S., Medlyn, B. E., De Kauwe, M. G., Walker, A. P., Dietze, M. C., Hickler, T., et al. (2014). Evaluation of 11 terrestrial carbon-nitrogen cycle models against observations from two temperate free-air CO_2 enrichment studies. *New Phytologist*, *202*(3), 803–822. https://doi.org/10.1111/nph.12697

Zamani, S., & Mahmoodabadi, M. (2013). Effect of particle-size distribution on wind erosion rate and soil erodibility. *Archives of Agronomy and Soil Science*, *59*(12), 1743–1753. https://doi.org/10.1080/03650340.2012.748984

Zhang, C., Zou, X., Gong, J., Liu, L., & Liu, Y. (2004). Aerodynamic roughness of cultivated soil and its influences on soil erosion by wind in a wind tunnel. *Soil and Tillage Research*, *75*(1), 53–59. https://doi.org/10.1016/S0167-1987(03)00159-4

Zhang, Q., Pitman, A. J., Wang, Y.-P., Dai, Y. J., & Lawrence, P. J. (2013). The impact of nitrogen and phosphorous limitation on the estimated terrestrial carbon balance and warming of land use change over the last 156 yr. *Earth System Dynamics*, *4*(2), 333–345. https://doi.org/10.5194/esd-4-333-2013

Zhang, Q., Wang, Y.-P., Pitman, A. J., & Dai, Y. J. (2011). Limitations of nitrogen and phosphorous on the terrestrial carbon uptake in the 20th century. *Geophysical Research Letters*, *38*, L22701. https://doi.org/10.1029/2011GL049244

Zhang, X., Rayner, P. J., Wang, Y.-P., Silver, J. D., Lu, X., Pak, B., & Zheng, X. (2016). Linear and nonlinear effects of dominant drivers on the trends in global and regional land carbon uptake: 1959 to 2013. *Geophysical Research Letters*, *43*, 1607–1614. https://doi.org/10.1002/2015GL067162

Zhao, D., Reddya, K. R., Kakania, V. G., & Reddy, V. R. (2005). Nitrogen deficiency effects on plant growth, leaf photosynthesis, and hyperspectral reflectance properties of sorghum. *European Journal of Agronomy*, *22*(4), 391–403. https://doi.org/10.1016/j.eja.2004.06.005